Towards a better understanding of vinylene carbonate derived SEI-layers by synthesis of reduction compounds

Sylvie Grugeon, Piotr Jankowski, Dominique Cailleu, Coralie Forestier, Lucas Sannier, Michel Armand, Patrik Johansson, Stéphane Laruelle

Towards a better understanding of vinylene carbonate derived SEI-layers by synthesis of reduction compounds

Sylvie Grugeon[ab], Piotr Jankowski[deg], Dominique Cailleu[c], Coralie Forestier[abfg], Lucas Sannier[bfg], Michel Armand[a], Patrik Johansson[eg] and Stephane Laruelle[ab*]

[a]*Laboratoire de Réactivité et Chimie des Solides, CNRS UMR 7314, Université de Picardie Jules Verne, 33 rue Saint Leu, 80039 Amiens, France*
[b]*Réseau sur le Stockage Electrochimique de l'Energie, CNRS RS2E FR3459, France*
[c]*Plate-Forme Analytique, Université de Picardie Jules Verne, 33 rue Saint Leu, 80039 Amiens, France*
[d]*Warsaw University of Technology, Faculty of Chemistry, 00-664 Warszawa, ul. Noakowskieg 3, Poland*
[e]*Department of Physics, Chalmers University of Technology, SE-412 96 Gothenburg, Sweden*
[f]*Renault, DEA-IREB, Technocentre, 1 avenue du Golf, 78288 Guyancourt, France*
[g]*ALISTORE-ERI European Research Institute, CNRS FR 3104, Hub de l'Energie, Rue Baudelocque, 80039 Amiens, France*

[*]*corresponding author : stephane.laruelle@u-picardie.fr*
Tel : +33 322825778

ABSTRACT

Here two chemical reduction pathways to synthesize the vinylene carbonate (VC) and poly(VC) reduction products are investigated, with the precise aim of further deciphering the lithium-ion battery solid electrolyte interphase (SEI) layer composition and the associated reduction mechanisms. The liquid synthesis pathway offers the opportunity of varying the concentration of Li-4,4'-Di-tert-butylbiphenyl reducing agent, whereas the dry synthesis pathway by ball milling allows to solve issues related to solvent-induced side reactions and washing procedure. As a result, the two syntheses do not unveil the same reduction mechanisms, favouring either carboxylate or carbonate salts as the major end product. The latter pathway is very efficient in terms of providing SEI-layers products resulting in well-defined IR spectra and comparisons with simulated spectra enable us to obtain IR fingerprints of the Li di-vinylene di-carbonate (LDVD) compound. Taken together the synthesis procedures provide information on conditions favouring radical polymerisation and further poly(VC) reduction into Li_2CO_3 and polyacetylene. Overall, this chemical simulation of SEI-layers formation assists in a proper characterization of the SEI-layers created on graphite surfaces by their IR spectra showing that Li_2CO_3, LDVD and poly(VC) are all present in different proportions dependent on the VC content in the electrolyte.

Keywords: Li-ion battery, SEI, additive, vinylene carbonate, ball milling, IR

1. Introduction

Besides issues related to climate change, our ever increasing dependence on non-renewable fossil resources constitutes a potential vulnerability to our way of living and is furthermore a likely source of socio-political and economic instability. Therefore, supporting sustainable development and diversifying our energy supply are both urgently required for the well-being of future generations. In this context, high energy density Li-ion batteries (LIBs) have become an obvious choice for powering electric vehicles and portable electronics, and are emerging also for large-scale energy storage of renewable energy such as solar, wind and wave power – but this can only succeed if they can meet the durability requirements for each of these applications. The latter is still a challenge, requiring a comprehensive knowledge of LIB aging processes upon cycling as well as by calendar life, why extensive studies aim at defining both best materials/components and their operating conditions. Inside the cells, aging of LIBs always involves resistive/capacitive contributions at the electrode/electrolyte interfaces, from active materials developing cracks from repeated swelling phenomena upon lithiation/delithiation processes and by the evolution of the solid electrolyte interphase (SEI), an electronically insulating but ionically conducting passivation layer at the negative electrode surface, a concept introduced by Peled in 1979 [1]. The SEI consists of lithium salts formed from electrolyte reduction processes at the negative electrode [2]; a reduction unavoidable as the LIB cycling potential range exceeds the electrolyte electrochemical stability window. The SEI is imperative to LIB functionality and is therefore also always artificially reinforced to, at least to some degree, extend the cycle life e.g. by electrolyte additives reduced prior to the electrolyte solvents and creating better SEIs.

However, understanding the role(s) played by the electrolyte additive(s) remains a key challenge - we still do not know the specific SEI properties responsible for a more stable cycling lifetime and foremost not the details of the initial reduction processes that ultimately will control the composition and morphology of the SEI. Therefore, whether a SEI-forming additive is beneficial or not to cell performance is always deduced from battery cycling, a cumbersome trial-and-error process. Vinylene carbonate (VC) was one of the first SEI-forming additives which showed a genuine enhanced LIB cycling stability improvement [3–5], but only when added in an appropriate amount; too much VC increases the battery impedance [6,7]. Since the early 2000's, much research effort has been devoted to the computational determination of reduction voltages [8–12] to enable predictive screening for suitable SEI-forming additives to subsequently be tested. At the same time, experimental state-of-the-art surface analysis

techniques such as infrared (IR) [6,13–20], X-ray photoelectron (XPS) [6,14–24] and nuclear magnetic resonance spectroscopies (NMR) spectroscopies [15,16,19,25,26] and time-of-flight secondary ion mass spectrometry (TOF-SIMS) [15] have been implemented to provide precise information on the composition of the nano-metric thick SEIs. The computations of reduction potentials are sensitive to the system choices and the environment i.e. lithium cations and solvent(s) as well as to whether the reactions follow the first or second electron reduction path, and therefore the literature is sometimes inconsistent. Results from the gas phase calculations are far away from the experimentally observed potentials, predicting values up to 2.76V *vs.* $Li^+/Li°$ [10] and showing the necessity for accounting solvent surroundings [9,11]. Depending on the choice of the methodology (functional, basis set, solvation model), computations show values in the 0.57-1.21V *vs.* $Li^+/Li°$ range [9,11,12]. Experimentally, however, it is clear that the general trend is that VC undergoes reduction at a higher potential than their saturated counterparts, i.e. the cyclic and linear electrolyte solvents. This results in a SEI with presence of polymeric species, and albeit more challenging in term of characterization, also lithium salts such as: i) unsaturated lithium alkyl di-carbonate salts, namely, lithium vinylene di-carbonate (LVD) $(=CH–OCO_2Li)_2$ and lithium di-vinylene di-carbonate (LDVD) $(–CH=CH–OCO_2Li)_2$, ii) lithium alkylene carbonate such as lithium vinylene carbonate (LVC) $CH_2=CH–OCO_2Li$, iii) lithium carboxylates such as lithium oxalate ($Li_2C_2O_4$) and lithium formate (HCO_2Li), and iv) lithium alkoxide likely participate to the formation of the SEI. Lithium carbonate (Li_2CO_3) was clearly identified in most of studies.

Overall, though carefully conducted, the large body of investigations still constitute a base for uncertainty with respect to the reduction mechanism of VC. Capturing the VC-derived SEI composition is indeed still challenging - quite understandable when considering the many additional processes involved as dissolution, reformation caused by active material volume expansion, etc., all making the composition and structure to evolve with time. Furthermore, a multi-layered/tapered structure/composition is likely as the surface chemistry and potential, hence the availability of electrons or additive molecules, gradually change across the film.

Here a detailed study of the infrared spectra signatures obtained for different VC reduction pathways has been performed:

i) reduction in solution via a radical anion (henceforth “solution synthesis”)
ii) reduction via a ball milling procedure in presence of metallic lithium (“ball milling synthesis”)
iii) electrochemical reduction at the graphite surface (“SEI-formation”)

and with additional support CP-MAS 13C NMR spectra analysis, we add to the body of knowledge and hopefully shed some new light on the VC reduction-derived SEI composition and the associated reaction mechanisms.

2. Experimental

2.1. Materials

All reagents were used as received, without further purification and manipulated inside an argon-filled glovebox (H_2O <0.1 ppm, O_2 <0.1 ppm). Vinylene carbonate (≤2% butylated hydroxytoluene, 97%), lithium metal, anhydrous tetrahydrofuran (≥99.9%), 2,2′-azo-bis(2-methyl-propionitrile) (AIBN, 98%) and 1,2 dimethyl-imidazole (98%) were all purchased from Sigma-Aldrich. 4,4'-Di-tert-butylbiphenyl (DBB, 99%) was supplied by Alfa Aesar. The battery-grade electrolyte and dimethyl carbonate were purchased from BASF, Germany.

2.2. Solution synthesis of polyvinylene carbonate (poly(VC))

Poly(VC) was prepared by mixing 3 mM of VC and 0.3 mM of the radical initiator AIBN. The mixture was left stirring for 12 hours at 70°C. The precipitate was purified through a solubilization-precipitation process using acetone and ethanol as solvent/non-solvent respectively. The resulting precipitate was vacuum dried at 80°C for 2 days prior to transfer into the glovebox.

2.3. Synthesis of VC and poly(VC) reduction products using a reducing agent

A Li-DBB radical anion, generated by reduction of DBB using 1 equiv. of Li metal in 0.3 mL THF solution, was used as reducing agent. The solution was left stirring for 4 h until the complete disappearance of the lithium metal, whereafter the desired amount of VC diluted in a THF solution was immediately added to the freshly prepared dark green reducing agent solution. A brown precipitate resulted, which was centrifuged and washed several times with THF before being vacuum dried overnight in the glovebox antechamber under argon atmosphere. Poly(VC) was also reduced in a similar way, except that it has been solubilized in a solution of 1,2 dimethylimidazole/THF prior to introducing the reducing solution.

2.4. Ball milling synthesis of VC, poly(VC), and EC reduction products

These syntheses were carried out using a Spex® 8000M mixer mill. The container and the ball were both made of stainless steel. VC with 2 equiv. of Li metal or EC with 1 equiv. of

Li metal were loaded with the ball into the container inside the argon-filled glovebox. The reagents were milled for 1h whereafter the container was opened inside the glovebox. The reactions were incomplete and residual VC and EC were evaporated under vacuum at room temperature. The black products still contained residual lithium metal and hence were extremely air-sensitive. Poly(VC) was ball-milled with 2 equiv. of Li metal under hexane. After disassembling the container inside the glovebox, the hexane was evaporated overnight in the glovebox antechamber under argon atmosphere.

2.5. SEI-formation at graphite surface

Swagelok®-type half-cells were assembled in the argon-filled glovebox. The working electrode consisted in 9 mg of synthetic graphite powder provided by SGL Carbon GmbH (d_{50} = 14 µm, S_{BET} = 6.5 $m^2.g^{-1}$) used as active material mixed in a mortar with conductive Super P carbon black (Timcal) in a 9:1 weight ratio respectively. Metallic lithium was used as counter and reference electrodes. The separator consisted of 1 microporous Celgard® membrane of polypropylene placed over the composite powder and 1 Whatman® membrane of glass fibre, both being supplied by GE Healthcare. Membranes and powder were impregnated with 90µL of electrolyte.

After a 2 h electrolyte soaking period, the cell was galvanostatically charged (graphite lithiation) and discharged (graphite delithiation) at 20°C between 0.005 and 1.5 V, at a rate of C/30, using a VMP-3 potentiostat-galvanostat (Biologic). The cell was disassembled inside the glovebox and the discharged graphite powder was scraped from the top of the current collector. The powder was then rinsed three times with battery-grade DMC to remove traces of electrolyte components and then vacuum dried under argon atmosphere overnight in the glovebox antechamber.

2.6. Chemical structure characterization

The ^{13}C NMR spectra were collected at 125 MHz under magic-angle spinning conditions (MAS) with a Bruker Avance III console and a 4 mm BB-1H MAS probe. All the samples were packed into the 4 mm zirconia rotors. Solid-state ^{1}H-^{13}C cross polarization magic-angle spinning (CP/MAS) NMR spectra were acquired at MAS frequency of 9 kHz using a cross-polarization sequence with a contact time of 1 ms and a recycle delay of 5 s. Specific ^{13}C spectra were recorded with a single pulse 45° sequence with recycle delay of 600 s. Fourier transform IR spectra were collected in transmission mode using a Nicolet 6700. KBr pellets were prepared in the glovebox and placed inside a plastic bag -which was opened in the N_2-

purged sample chamber of the FTIR spectrometer just prior to the analysis. Spectra were averaged from 64 scans with a resolution of 4 cm^{-1}.

2.7. Simulation of IR spectra

Vibrational frequencies, modes and corresponding IR intensities for a set of geometry optimized molecules representing SEI-forming additives, solvents, and likely SEI-layer components were computed by DFT using the M06-2X functional and the 6-311++G(d,p) basis set, as implemented in Gaussian09 [27]. A C-PCM solvation model with parameters for water was used, as a good approximation of any high dielectric ($\varepsilon > 20$) solvent [REF#11]. To better compare the calculated IR data with the experimental data a frequency scaling factor of 0.96 was applied [28].

3. Results and discussion

3.1. Solution synthesis

VC reduction. Owing to its thinness and air-sensitivity, the IR spectra analysis of SEI-layers is intrinsically tricky, and relying on additional reduction products synthesis to assist in the interpretation of the results has already proven effective [28]. Assuming that a reduction via reaction with radical anion mimics a reduction process occurring in a LIB, Michan *et al.* [19] used 1 and 0.5 equiv. of the lithium naphtalenide reducing agent (-2.5 V *vs.* NHE) to reduce VC. In their both IR spectra, lithium carbonate (Li_2CO_3) was identified through the bands at 1488, 1449 and 878 cm^{-1}. Based on comparison with spectra related to previous studies, their peaks for carbonate C=O (1793 cm^{-1}) and C–O (1077, 1172 cm^{-1}) were assigned to radical polymerization derived poly(VC) and for carboxylate C=O (1660/1600 cm^{-1}) and C–O (1428 cm^{-1}) to HCO_2Li/$Li_2C_2O_4$; the presence of such compounds being corroborated by their multinuclear solid-state NMR and XPS analyses. They also showed that reducing the lithium naphtalenide amount from 1 to 0.5 equiv. leads to less intense Li_2CO_3, $Li_2C_2O_4$ and HCO_2Li bands as compared to the C=O (1793 cm^{-1}) peak assigned to poly(VC), thus unveiling a Li concentration dependence in the formation of such inorganic/organic species. Through ^{13}C NMR analysis, the repeating ethylene carbonate (EC) units of poly(VC) was clearly identified with the characteristic peaks at 155 and 74 ppm assigned to $ROCO_2R$ and CHO, respectively. Interestingly, owing to the presence of a peak at 100 ppm related to $CH(OR)_2$, the possibility of a cross-linking site for poly(VC) was put forward and explained to be due to the formation

of the intermediate unsaturated vinyloxy radical (C_2H_3O•) resulting from successive VC reduction, decarboxylation and protonation processes. The lithium inorganic Li_2CO_3, $Li_2C_2O_4$ and organic HCO_2Li salts with corresponding peaks at resp. 170, 172 and 179 ppm were proposed to be formed from reduction of CO_2, the latter being released, as above described, just after the radical anion generation.

This outstanding contribution to the knowledge of VC reduction mechanisms incited us to go further and expand the study to the role of reducing agent equivalents from 0.2 up to 2.5 so as to promote VC reduction via a subsequent 2-electron reduction path. Li-DBB [29] was chosen as reagent agent as it is known to generate sensitive alkyllithium reagents at low temperature, with higher yields than other reagents, at ca. -2.4 V vs NHE. 0.2, 1.0, 2.0 and 2.5 equiv. of this Li-DBB in THF solution were used to reduce VC. After thorough washing, procedure, the resulting powders were characterized by IR spectroscopy (Fig.1) – resulting in peaks related to poly(VC) at 1818, 1261, 1171, 1076, 770 and 722 cm^{-1} steadily decreasing with increasing Li-BDD equiv., up to a complete disappearance for 2.5 equiv.. This result corroborates the above-reported results with 0.5 and 1 equiv., and poly(VC) formation through radical polymerization is suggested to be promoted when the lower reducing agent amounts are available. We can assume that due to the low production of VC radical anions, the recombination reaction to produce lithium alkyl salts is prevented, thus favoring a radical polymerization process. In addition to the poly(VC), some peaks for Li_2CO_3 are observed at 1505, 1432 and 876 cm^{-1}. These peaks seem slightly attenuated with increasing amounts of reducing agent, whereas the large band in the 1600-1670 cm^{-1} range dominates - ascribed to C=O of $Li_2C_2O_4$/HCO_2Li as suggested above and/or to C=O of lithium alkyl carbonates whose peak at 827 cm^{-1} (ω_{OCO2}) demonstrates its presence [30,31]. The small peak at 784 cm^{-1}, only well distinguishable in the absence of poly(VC), could be assigned to $Li_2C_2O_4$ and/or HCO_2Li. These compounds should also resonate in the 1300-1400 cm^{-1} range, which here could correspond to the 1320 or 1374 cm^{-1} peaks.

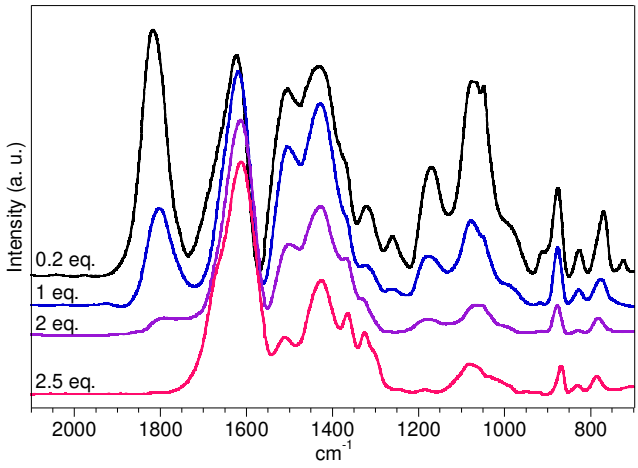

Fig. 1: IR spectra of VC reduced compounds obtained from solution synthesis with different LiDBB equiv.

Though some tendencies regarding poly(VC) and lithium salts evolution as a function of reducing agent molar concentration can be highlighted, achieving a complete assignment of the all the peaks remains a difficult task. Hence, as a complementary technique, ^{1}H-^{13}C CP/MAS NMR measurements were performed, but as shown in Fig.2, the spectra unfortunately show heavily overlapping and poorly resolved peaks. THF solvent with resonances at 27 and 70 ppm is still present in all samples despite the harsh drying procedure and residual DBB may contribute to the signals around 35 (CH_3) and 125 ppm (CH=CH). In accordance with previous NMR studies [19], the presence of residual solvent and reducing agent precursor molecules seems unavoidable and may give rise to misinterpretation of spectra. Indeed, all spectra display a broad resonance in the 125-135 ppm range, characteristic of C=C double bonds, but given the above, any unambiguous attribution to any VC reduction products such as unsaturated lithium alkyl carbonates is impossible, and is therefore here addressed by an organic molecule-free synthesis of VC reduction products.

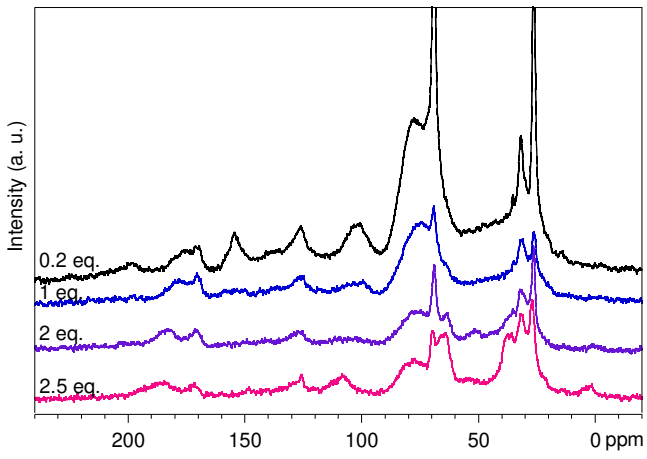

Fig. 2: ^{1}H-^{13}C CP/MAS NMR spectra of VC reduced compounds obtained from solution synthesis

with different LiDBB equiv.

Anyhow line with the IR analysis, the 0.2 equiv. NMR spectrum displays distinct resonances at 154 and 77 ppm related to poly(VC) with resonances at ca. 100 and 32 ppm assigned to $CH(OR)_2$ and RCH_2R', respectively in the Michan *et al.*'s study [19]. They therefore suggested cross-linking of poly(VC) through the formation of intermediate CH_2CHO radicals. Apart from the peak around 32 ppm, the resonances pertaining to poly(VC) are less visible when using 1 equiv. value and not any more detectable for 2.0 and 2.5 equiv., in agreement with IR spectra analysis. In all of the NMR spectra, a signal at ca.171 ppm is observed, consistent with the presence of Li_2CO_3, as also observed in the IR spectra. Broader peaks appear up to 195 ppm, which suggest the presence of lithium carboxylates such as $Li_2C_2O_4$, HCO_2Li in various amounts. With 2.0 and 2.5 equiv., many other resonances are found: 129, 108, 80, 64 and 38 ppm. The attribution of these chemical shifts is rather difficult and would require a deeper study taking into account supplementary parasite reactions e.g. decomposition of the Li-BDD in THF solution [29] and hydrolysis. Indeed, we cannot rule out the presence of hydroxyl group containing compounds, which would have signals within the 60-90 ppm range and could be formed from lithium alkyl carbonates hydrolyzed by traces of water contained in the reagents. Furthermore, as poly(VC) was clearly evidenced for small amounts of the reduction agent, a legitimate is whether or not it is formed also in presence of large amounts of the reducing agent.

Poly(VC) reduction. The 2-electron reduction of separately synthesized poly(VC) was undertaken after solubilization in presence of 1,2 dimethyl-imidazole and using the same Li-DBB reagent. The dark-green reducing solution turned into pale brown as soon as the poly(VC) solution was introduced, demonstrating its possible reduction after solubilization at potential from ~0.6V *vs.* $Li^+/Li°$. The ^{13}C CP/MAS NMR spectrum (Fig. 3a) shows intense peaks at 70 and 63 ppm, generally attributed to primary and secondary alcohol moieties, at 30 and 36 ppm, within the alkyl carbon range, and at 174 and 183 ppm, indicative of COO or COOH functional groups. The presence of alcohol groups indicates the presence of a large amount of water, which entails parasitic reactions. Interestingly, a quite well-resolved peak at 170 ppm highlights the presence of Li_2CO_3 as also demonstrated in the IR spectra (Fig. 3b), and signals in the 120-150 ppm chemical shift region of carbon double bonds are also visible. These resonances lead us to assume that poly(VC) has undergone a 2-electron reduction to produce Li_2CO_3 and polyacetylene, as previously suggested by Armand [32]. These resonances are

absent in the VC reduction-related spectra obtained with large amounts of reducing agents, 2.0 and 2.5 equiv., supporting the assumption that poly(VC) does not form under these conditions.

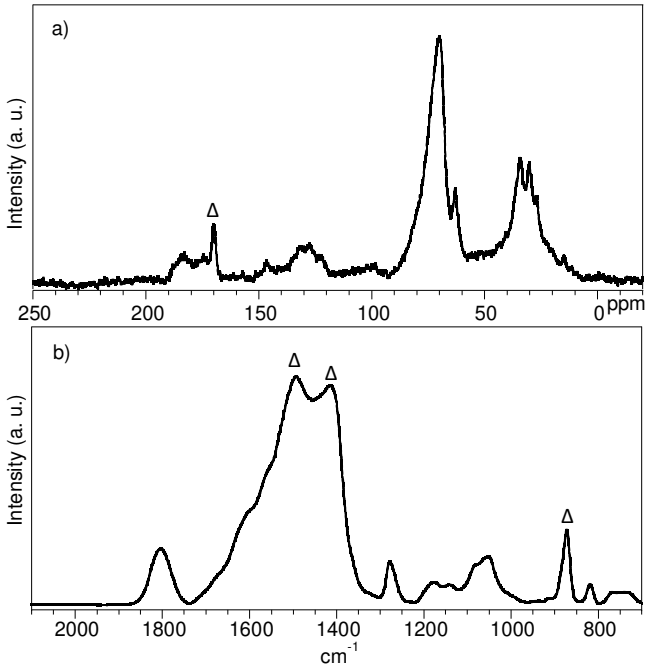

Fig. 3: a) ^{1}H-^{13}C CP/MAS NMR and b) IR spectra of poly(VC) reduced compound obtained from solution synthesis with 2 LiDBB equiv.

Overall, the reduction reaction through a reducing agent in solution proved to be very efficient on VC and solubilized poly(VC), leading to the formation of different products depending on the reducing agent amount. However, solid-state CP/MAS NMR and IR analysis did not allow us to achieve complete assignments of all of the signals owing to issues of resolution, overlaps, presence of residual reagents, and most also likely parasitic reactions from water and relative stability of reagents. Therefore, further investigations using an organic reagents-free ball milling process were conducted.

3.2. Ball milling synthesis

VC reduction. The ball milling synthesis of VC was carried out with 2 equiv. of metallic lithium. Supported by the fact that VC additive-derived SEI compounds are known to provide a highly passivating SEI-layer, the reaction yield was very poor, ca.10%, for both milling times, 1 and 2 h, why there was no reason to vary the reducing agent amount. The reaction product was highly divided lithium surrounded by a passivating layer and residual VC. The latter was

evaporated under vacuum either just after the end of the ball milling procedure ("initial") or 3 h later. The residual black powders were first subjected to a careful IR analysis (Fig. 4).

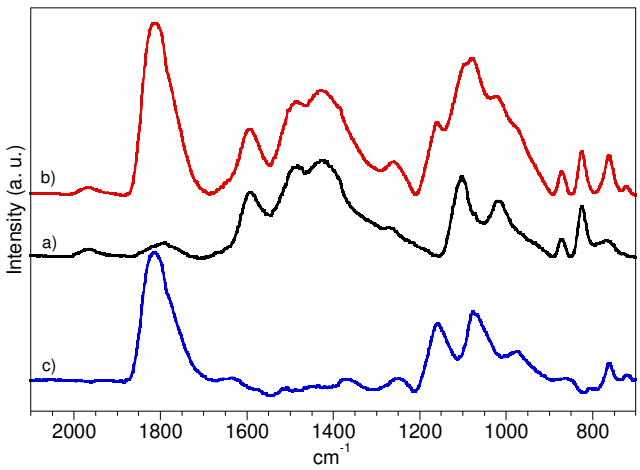

Fig. 4: IR spectra of VC reduced compounds obtained from ball milling synthesis a) without resting time b) with 3 h resting time and c) resulting spectrum obtained from a)-b) subtraction.

The initial sample displays a band at 1814 cm^{-1} of relatively low intensity suggesting the presence of a small amount of poly(VC) (Fig. 4a). After 3 h of resting time before VC evaporation, this band was found to be present with an increased intensity (Fig. 4b). The IR profile resulting from subtraction of the initial spectrum matches well with synthesized poly(VC) with major bands at 1814, 1157, 1078, 762 and 719 cm^{-1} (Fig. 4c) - hence the initial ball-mill built SEI-layer is well preserved for at least 3 h. However, it allows further VC reduction, but with such a limited lithium availability that recombination processes are prevented. The radical polymerization process is thus favored similarly to the case of the solution synthesis utilizing a limited amount of reducing agent. The initial passivation layer (Fig. 4a or 5a) clearly shows the presence of Li_2CO_3 with characteristic bands at 1485, 1428 and 871 cm^{-1} as well as quite well-resolved peaks at 1593, 1102, 1023 and 825 cm^{-1} and possibly a shoulder at 1395 cm^{-1} more visible after subtraction of the Li_2CO_3 spectra (Fig. 5b and 5c).

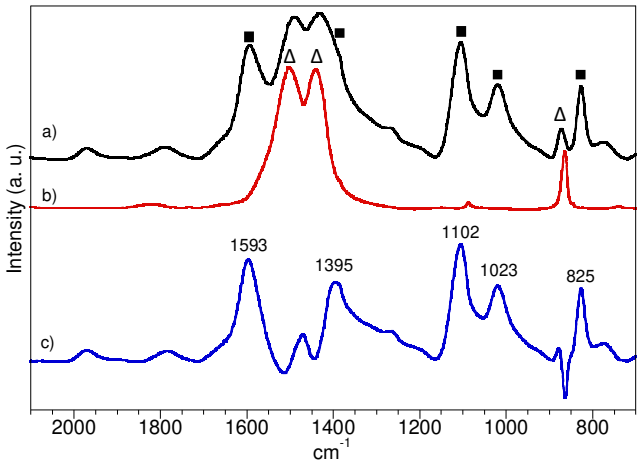

Fig. 5: IR spectra of a) VC reduced compounds obtained from ball milling synthesis without resting time b) poly(VC) reduced compounds obtained from ball milling synthesis - this spectrum is also used as Li_2CO_3 reference spectrum and c) resulting spectrum obtained from a)-b) subtraction.

Among the DFT simulated possible products of the VC reduction, unsaturated di-carbonates such as lithium vinylene di-carbonate (LVD) $(=CH–OCO_2Li)_2$ and lithium divinylene di-carbonate (LDVD) $(–CH=CH–OCO_2Li)_2$, show signals in the same range (Table 1). Especially the LDVD data matches the experimental data well, within 14-39 cm^{-1} for the four main peaks. Thus we can speculate that these peaks could all originate from LDVD. The presence of such unsaturated lithium alkyl carbonates was already suggested in case of solution synthesis due to a contribution in the 1600-1670 cm^{-1} range and at 825 cm^{-1} (Fig. 1). The initial spectrum (Fig. 4a or 5a) also exhibits a peak at 1968 cm^{-1} which was seen in the literature in spectra obtained from the surface of alkalinized Pt catalysts and assumed to be the result of an electrostatic attraction of C=O with alkali cations lowering the stretching frequency [33]. We make the assertion that any residual surface lithium species could produce the very same effect. To summarize, the IR spectrum of VC reduced through ball milling with lithium metal reveals the presence of Li_2CO_3 and another component that might be a lithium divinylene di-carbonate. The ^{1}H-^{13}C CP/MAS NMR spectrum (Fig. 6a) depicts a main broad peak centered around 130 ppm within the C=C chemical shift region, which corroborates our assumption that VC ball milling synthesis would form, among other components, unsaturated lithium alkyl carbonates. Note that C nuclei of terminal vinyl group $=CH_2$ are expected to absorb within the 110-120 ppm chemical shift interval. The absence of resonances in this region rules out the presence of lithium vinylene carbonate (LVC) $CH_2=CH–OCO_2Li$ [13]. Surprisingly, the resonance from Li_2CO_3 and presumed $ROCO_2Li$ at 171 and 160 ppm, respectively, could not be detected, which can be, however, explained by the too low product amount; the sample is also composed of residual lithium metal.

Assignment	Wavenumbers [cm^{-1}]		
	calculated LVD[a]	calculated LDVD[a]	experimental
$\delta_{o.o.p.\ OCO_2}$	896	840	825
ω_{C-H}	927	984	1023
$\nu_{o.o.p.\ O-C_{(=C)}}$	1121	1088	1102
ρ_{C-H}	1228	1213	
$\nu_{asym.\ OCO_2} + \rho_{C-H}$		1287	
$\nu_{sym.\ OCO_2} + \nu_{C=C}$	1311	1328	1395
$\nu_{asym.\ OCO_2} + \nu_{C=C}$	1669	1618	1593

[a] scaled by 0.96

Table 1: The main vibrational modes for LVD and LDVD; computed and experimental wavenumbers.

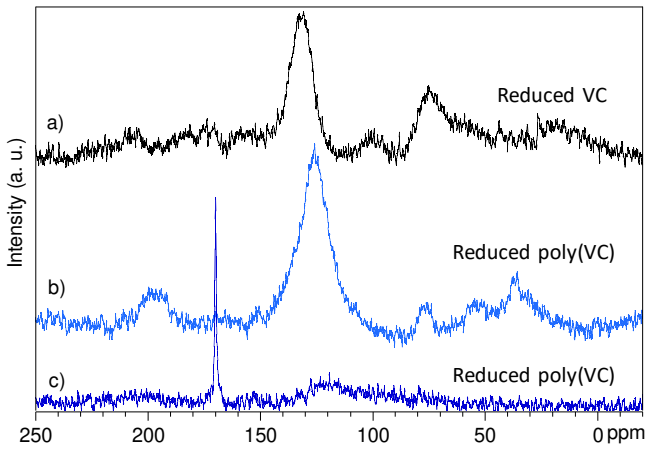

Fig. 6: ^{1}H-^{13}C CP/MAS NMR spectra of a) VC, b) poly(VC) reduced compounds obtained from ball milling synthesis and c) ^{13}C NMR spectrum of poly(VC) reduced compounds obtained from ball milling synthesis.

Poly(VC) reduction. Synthesized poly(VC) was ball-milled with 2 equiv. of metallic lithium for 1 h. The IR spectrum (Fig. 5b) only reveals well-defined peaks corresponding to Li_2CO_3 at 1500, 1435, 1088 and 865 cm^{-1}. This impies that the 2-electron reduction reaction of poly(VC) is complete and leads to Li_2CO_3 and obviously polyacetylene as mentioned above, despite that the IR spectrum does not exhibit the polyacetylene peaks, namely at 3013 and 1013 cm^{-1} or 1251 and 740 cm^{-1}, corresponding to the trans and cis isomers, respectively. In contrast, the ^{1}H-^{13}C CP/MAS NMR spectrum (Fig. 6b) shows a main broad peak centered at 126 ppm, a spectral range wherein the C=C units of cis-polyacetylene resonate [34], but here the Li_2CO_3 peak at 171 ppm is absent, suggesting its ^{13}C nuclei are separated enough from ^{1}H of polyacetylene to hinder any cross polarization. However, the ^{13}C NMR spectrum (Fig. 6c) does reveal a sharp peak from Li_2CO_3 along with a barely visible broad peak within the 110-130 ppm range.

To summarize, both the solution and ball-milling routes to synthesize VC and poly(VC) reduction products provides further insight and show that the methods favor different VC reduction reaction pathways. VC radical polymerization process was found to prevail over recombination reaction for low amounts of LiDBB. Despite of overlapping and broad bands, Li_2CO_3, lithium alkyl carbonates, and carboxylates; oxalate and/or formate, were identified. The major issue is that this reduction protocol is prone to bring about side reactions, something which is circumvented in the ball milling reduction path – resulting in revealing the presence of Li_2CO_3 and LDVD. Once formed at the surface of the highly divided lithium powder, this carbonate salts containing layer seems to be stable over time whereas the amount of poly(VC) increases when kept in continuous contact with the residual VC-containing slurry. The carbonate salt layer restricts the access of VC to the lithium and thus favors the radical polymerization process (Eq. 1). The solid/liquid ball milling synthesis seems to promote formation of carbonate salts through C_{ether}-O bond cleavage (Eq. 2) whereas in the liquid/liquid solution synthesis with high amount of reducing agent, lithium cations can draw electrons from the carbonyl group and promote the $C_{carbonyl}$-O bond cleavage leading to the formation of carboxylate phases. The latter was suggested by Michan *et al.* [19] to be formed after one-electron VC reduction, from CO_2 gas reduction reaction, which is likely to be considered in this very reactive liquid media or they can be directly formed from a successive two-electron VC reduction (Eq. 3).

Poly(VC) turned out to also be reduced through both pathways, but only the ball-milling synthesis gave rise to IR spectra with well resolved bands characteristic of Li_2CO_3 as well as a broad ^{1}H-^{13}C CP/MAS NMR band within the C=C region that proves the presence of polyacetylene (Eq. 4).

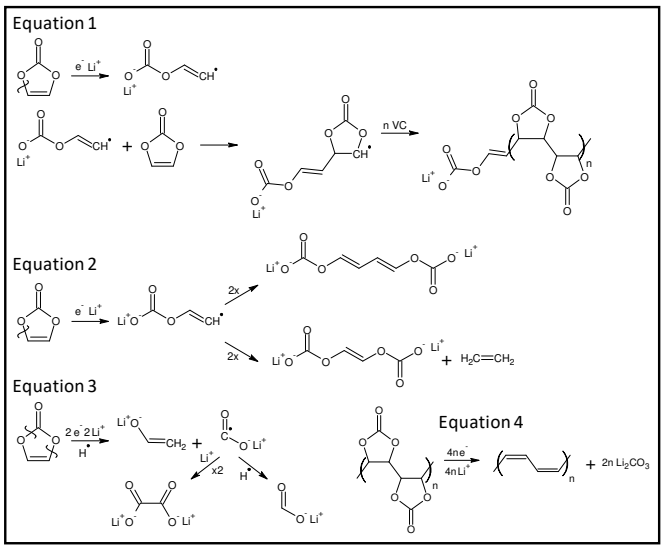

On the basis of all the above, the question arose as to whether the IR fingerprints of these VC reduction compounds IR fingerprints could help us to gain further insight into the characterization of the electrochemically formed SEI on graphite.

3.3. Characterization of the SEI formed on graphite surface

Graphite and Super P carbon composite electrodes were subjected to one lithiation-delithiation electrochemical process in half-cells with electrolytes of 1M $LiPF_6$ in either 100% VC, EC-DMC-EMC (1:1:1 vol. ratio) with or without 2 wt.% of VC, and the IR spectra obtained from the corresponding SEI-layers are shown in Figure 7-1.

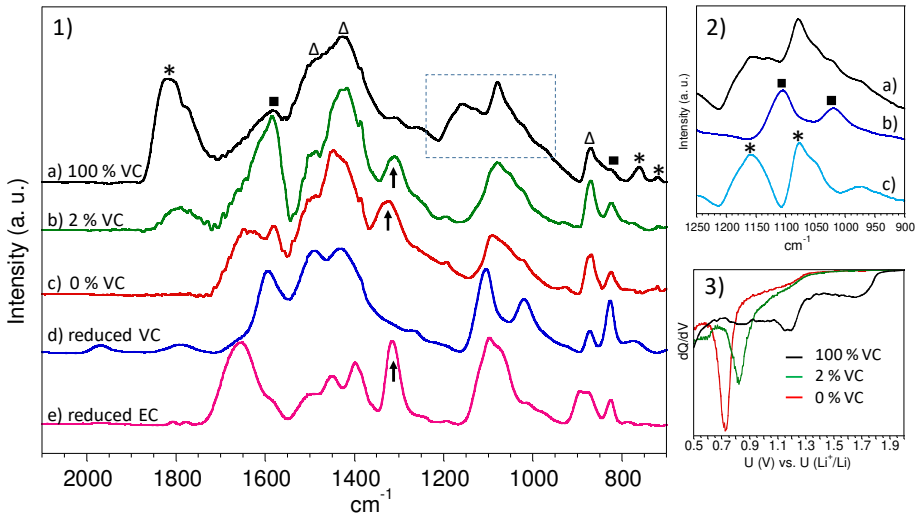

Fig. 7: 1) IR spectra of graphite SEI-layers formed in electrolyte with different percentage of VC and of VC and EC reduced compounds obtained from ball milling synthesis. 2) zoom of the a) 100 % VC spectrum b) reduced VC spectrum. c) resulting spectrum obtained from a)-b) subtraction. 3) ∂Q/∂V derivative curves of first graphite lithiation in electrolyte with different VC percentage.

For the electrodes cycled vs. the 1 M $LiPF_6$ in VC electrolyte, the IR spectrum (Fig. 7-1a) reveals peaks pertaining to Li_2CO_3 within the 1400-1500 cm^{-1} range and at 870 cm^{-1}, poly(VC) with bands in the 1750-1850 cm^{-1} range and at 760 cm^{-1}, and lithium alkyl carbonate with bands at ca. 1600 cm^{-1} and 825 cm^{-1}. Within the 900-1250 cm^{-1} range, the presence of the latter two compounds can also be deduced from a subtraction of the LDVD bands at 1102 and 1023 cm^{-1} (Fig. 7-2b) of the ball-milled VC compound. The resulting spectrum (Fig. 7-2c) reveals characteristic bands of poly(VC) at 1158 and 1078 cm^{-1}. This composition resembles that obtained after 1 h ball milling followed by 3 h resting time (Fig. 4b). As large amounts of electrons and thus radicals can be provided at the surface of the graphite particles, the SEI-layer when first formed is assumed to be mainly composed of LDVD and Li_2CO_3, from radical

recombination and two-electron reduction processes, respectively. Subsequently, poly(VC) forms in cracks SEI-layer, stemming from the volume expansion (ca. 10%) of the graphite particles and then propagates. Based on this assumption, VC continues to be reduced during the low potential graphite lithium intercalation plateaus and furthermore in contact with the active material surface, poly(VC) may also be reduced to Li_2CO_3 and polyacetylene - which can be reduced up to 1 Li per 9 C, $CHLi_{0.111}$ or $(C_3H_3)_3Li$, and create n-doped polyacetylene [35].

The electrodes cycled vs. the EC-DMC-EMC with 2 wt.% VC electrolyte result in a SEI-layer with an IR spectrum (Fig. 7-1b) featuring Li_2CO_3, a minor poly(VC) contribution, as compared to the VC electrolyte, and a larger amount of Li alkyl carbonates. LDVD is present with a predominant band at ca. 1590 cm^{-1}. However, when compared with the IR spectra of the EC reduced compound obtained from ball milling with lithium (Fig. 7-1e) and of the SEI-layer obtained without VC (Fig. 7-1c), it is clear that EC also is reduced. Indeed, the relatively strong intensity of the CH_2 wagging mode peak at ca.1330 cm^{-1} and the shoulder around 1650 cm^{-1} prove the presence of Li ethylene di-carbonate [31]. The EC reduction can easily be envisaged from $\partial Q/\partial V$ derivative curves (Fig. 7-3) as the EC and VC reduction peaks are very close to each other, both in the 1- 0.6 V *vs.* Li^+/Li range. The limited amount of poly(VC) may be explained by the restricted presence of VC accessible to radicals within the SEI cracks. On the other hand, the primary layer composed of EC and VC reduced compounds may also display different passivation properties; larger ethylene-based Li alkyl di-carbonate species may accommodate the graphite volume expansion differently than vinylene-based species.

The transmission electron micrographs reported in a previous paper by some of us [36] showed a 10 nm thick smooth, uniform, and perfectly covering SEI-layer for graphite vs. a 2wt.% VC electrolyte – and to be much more homogeneous than a solvent reduction-induced SEI-layer (10-25 nm). Without VC, the DMC and EMC linear carbonate solvents reduce at the same time as EC [37], forming lithium methyl or ethyl carbonate and lithium methoxide or ethoxide [38], which are all more soluble than the di-salts resulting from EC and VC reduction. Moreover, the alkoxide anions can trigger formation of oligomers through a succession of nucleophilic attacks [39] which can be deleterious for the battery performance, but in the presence of VC, this reduction is hindered [37]. Increasing the VC amount increases the reduction potential which can hinder EC reduction and favor the formation of poly(VC), especially in cracks or on top of the carbonate salt-based layer. Too much poly(VC) may also be deleterious [40], as it may increase battery impedance.

4. Conclusion

Two synthesis routes to obtain VC and poly(VC) reduction compounds have been successfully implemented and subsequent IR and NMR spectroscopy have provided valuable data to analyze both the SEI composition and the associated reaction mechanisms. The solvent-less ball milling synthesis is proposed to solve the issues related to the solution synthesis such as side reactions and the washing procedure. Hereby, it offered the opportunity to obtain a well-resolved LDVD IR spectrum. Both the solution and ball milling syntheses yielded poly(VC) using VC radicals-lean media. This supposes that, in presence of a VC-rich electrolyte, graphite lithiation initially leads to radicals recombination processes at the surface of the graphite particles to generate lithium alkyl carbonates and lithium carbonate, and subsequently poly(VC) forms within graphite volume expansion-derived SEI cracks before further propagating on top of this primary SEI-layer. The solution synthesis unveiled the tendency to preferably reduce VC into carboxylate-type species in the presence of large amounts of reducing agent, indicating that the presence of a large quantity of Li cations favors O-CO cleavage. Poly(VC) has also been reduced through both synthesis routes leading to Li_2CO_3 and polyacetylene – hence both species can be envisaged in the SEI-layer if poly(VC) is localized at the extreme surface of the active materials. On the other hand, the IR spectra of the SEI-layer on graphite formed using a 2 wt.% VC containing carbonate-based electrolyte seems to indicate that both VC and EC are reduced which can explain differences in the SEI compositions reported in the literature. Though these results deserve more detailed investigations as a function of cycling and ageing conditions as well as of synergetic effects in the presence of other additives, the present synthesis and electrochemistry-focused approach has proven to be relevant and successful, and paves the way for further studies dedicated to improve the lifespan of LIBs.

ACKNOWLEDGMENTS

Support from the Association Nationale de la Recherche et de la Technologie (ANRT, France) is gratefully acknowledged. Calculations have been carried out at the Wroclaw Centre for Networking and Supercomputing (http://www.wcss.pl), grant No. 346. The support by Chalmers Area of Advance Energy for a travel scholarship to Piotr Jankowski is gratefully acknowledged. Patrik Johansson acknowledges both the Swedish Energy Agency for a basic

research grant via the Swedish Research Council and the continuous support by many of Chalmers Areas of Advance: Energy, Materials Science, and Transport.

References

[1] E. Peled, The Electrochemical Behavior of Alkali and Alkaline Earth Metals in Nonaqueous Battery Systems—The Solid Electrolyte Interphase Model, J. Electrochem. Soc. 126 (1979) 2047–2051. doi:10.1149/1.2128859.

[2] E. Peled, S. Menkin, Review—SEI: Past, Present and Future, J. Electrochem. Soc. 164 (2017) A1703–A1719. doi:10.1149/2.1441707jes.

[3] H. Ota, K. Shima, M. Ue, J. Yamaki, Effect of vinylene carbonate as additive to electrolyte for lithium metal anode, Electrochimica Acta. 49 (2004) 565–572. doi:10.1016/j.electacta.2003.09.010.

[4] D. Xiong, J.C. Burns, A.J. Smith, N. Sinha, J.R. Dahn, A High Precision Study of the Effect of Vinylene Carbonate (VC) Additive in Li/Graphite Cells, J. Electrochem. Soc. 158 (2011) A1431. doi:10.1149/2.100112jes.

[5] D. Pritzl, S. Solchenbach, M. Wetjen, H.A. Gasteiger, Analysis of Vinylene Carbonate (VC) as Additive in Graphite/LiNi0.5Mn1.5O4 Cells, J. Electrochem. Soc. 164 (2017) A2625–A2635. doi:10.1149/2.1441712jes.

[6] X. Zhang, C. Fan, P. Xiao, S. Han, Effect of vinylene carbonate on electrochemical performance and surface chemistry of hard carbon electrodes in lithium ion cells operated at different temperatures, Electrochimica Acta. 222 (2016) 221–231. doi:10.1016/j.electacta.2016.10.149.

[7] D.Y. Wang, N.N. Sinha, J.C. Burns, C.P. Aiken, R. Petibon, J.R. Dahn, A Comparative Study of Vinylene Carbonate and Fluoroethylene Carbonate Additives for $LiCoO_2$ /Graphite Pouch Cells, J. Electrochem. Soc. 161 (2014) A467–A472. doi:10.1149/2.001404jes.

[8] A. Wang, S. Kadam, H. Li, S. Shi, Y. Qi, Review on modeling of the anode solid electrolyte interphase (SEI) for lithium-ion batteries, Npj Comput. Mater. 4 (2018). doi:10.1038/s41524-018-0064-0.

[9] Y. Wang, P.B. Balbuena, Theoretical Insights into the Reductive Decompositions of Propylene Carbonate and Vinylene Carbonate: Density Functional Theory Studies, J. Phys. Chem. B. 106 (2002) 4486–4495. doi:10.1021/jp014371t.

[10] Y. Wang, S. Nakamura, K. Tasaki, P.B. Balbuena, Theoretical Studies To Understand Surface Chemistry on Carbon Anodes for Lithium-Ion Batteries: How Does Vinylene Carbonate Play Its Role as an Electrolyte Additive?, J. Am. Chem. Soc. 124 (2002) 4408–4421. doi:10.1021/ja017073i.

[11] P. Jankowski, W. Wieczorek, P. Johansson, SEI-forming electrolyte additives for lithium-ion batteries: development and benchmarking of computational approaches, J. Mol. Model. 23 (2017). doi:10.1007/s00894-016-3180-0.

[12] S.A. Delp, O. Borodin, M. Olguin, C.G. Eisner, J.L. Allen, T.R. Jow, Importance of Reduction and Oxidation Stability of High Voltage Electrolytes and Additives, Electrochimica Acta. 209 (2016) 498–510. doi:10.1016/j.electacta.2016.05.100.

[13] X. Zhang, R. Kostecki, T.J. Richardson, J.K. Pugh, P.N. Ross, Electrochemical and Infrared Studies of the Reduction of Organic Carbonates, J. Electrochem. Soc. 148 (2001) A1341–A1345. doi:10.1149/1.1415547.

[14] D. Aurbach, K. Gamolsky, B. Markovsky, Y. Gofer, M. Schmidt, U. Heider, On the use of vinylene carbonate (VC) as an additive to electrolyte solutions for Li-ion batteries, Electrochimica Acta. 47 (2002) 1423–1439. doi:10.1016/S0013-4686(01)00858-1.

[15] H. Ota, Y. Sakata, A. Inoue, S. Yamaguchi, Analysis of Vinylene Carbonate Derived SEI Layers on Graphite Anode, J. Electrochem. Soc. 151 (2004) A1659–A1669. doi:10.1149/1.1785795.

[16] M. Nie, J. Demeaux, B.T. Young, D.R. Heskett, Y. Chen, A. Bose, J.C. Woicik, B.L. Lucht, Effect of Vinylene Carbonate and Fluoroethylene Carbonate on SEI Formation on Graphitic Anodes in Li-Ion Batteries, J. Electrochem. Soc. 162 (2015) A7008–A7014. doi:10.1149/2.0021513jes.

[17] H.-H. Lee, Y.-Y. Wang, C.-C. Wan, M.-H. Yang, H.-C. Wu, D.-T. Shieh, The function of vinylene carbonate as a thermal additive to electrolyte in lithium batteries, J. Appl. Electrochem. 35 (2005) 615–623. doi:10.1007/s10800-005-2700-x.

[18] B. Zhang, M. Metzger, S. Solchenbach, M. Payne, S. Meini, H.A. Gasteiger, A. Garsuch, B.L. Lucht, Role of 1,3-Propane Sultone and Vinylene Carbonate in Solid Electrolyte Interface Formation and Gas Generation, J. Phys. Chem. C. 119 (2015) 11337–11348. doi:10.1021/acs.jpcc.5b00072.
[19] A.L. Michan, B.S. Parimalam, M. Leskes, R.N. Kerber, T. Yoon, C.P. Grey, B.L. Lucht, Fluoroethylene Carbonate and Vinylene Carbonate Reduction: Understanding Lithium-Ion Battery Electrolyte Additives and Solid Electrolyte Interphase Formation, Chem. Mater. 28 (2016) 8149–8159. doi:10.1021/acs.chemmater.6b02282.
[20] Z.L. Brown, S. Jurng, B.L. Lucht, Investigation of the Lithium Solid Electrolyte Interphase in Vinylene Carbonate Electrolytes Using Cu||LiFePO4 Cells, J. Electrochem. Soc. 164 (2017) A2186–A2189. doi:10.1149/2.0021712jes.
[21] M. Herstedt, A.M. Andersson, H. Rensmo, H. Siegbahn, K. Edström, Characterisation of the SEI formed on natural graphite in PC-based electrolytes, Electrochimica Acta. 49 (2004) 4939–4947. doi:10.1016/j.electacta.2004.06.006.
[22] L.E. Ouatani, R. Dedryvère, C. Siret, P. Biensan, S. Reynaud, P. Iratçabal, D. Gonbeau, The Effect of Vinylene Carbonate Additive on Surface Film Formation on Both Electrodes in Li-Ion Batteries, J. Electrochem. Soc. 156 (2009) A103–A113. doi:10.1149/1.3029674.
[23] J.-B. Gieu, C. Courrèges, L.E. Ouatani, C. Tessier, H. Martinez, Influence of Vinylene Carbonate Additive on the Li4Ti5O12 Electrode/Electrolyte Interface for Lithium-Ion Batteries, J. Electrochem. Soc. 164 (2017) A1314–A1320. doi:10.1149/2.0111707jes.
[24] Y. Qian, C. Schultz, P. Niehoff, T. Schwieters, S. Nowak, F.M. Schappacher, M. Winter, Investigations on the electrochemical decomposition of the electrolyte additive vinylene carbonate in Li metal half cells and lithium ion full cells, J. Power Sources. 332 (2016) 60–71. doi:10.1016/j.jpowsour.2016.09.100.
[25] A.L. Michan, G. Divitini, A.J. Pell, M. Leskes, C. Ducati, C.P. Grey, Solid Electrolyte Interphase Growth and Capacity Loss in Silicon Electrodes, J. Am. Chem. Soc. 138 (2016) 7918–7931. doi:10.1021/jacs.6b02882.
[26] Y. Jin, N.-J.H. Kneusels, L.E. Marbella, E. Castillo-Martínez, P.C.M.M. Magusin, R.S. Weatherup, E. Jónsson, T. Liu, S. Paul, C.P. Grey, Understanding Fluoroethylene Carbonate and Vinylene Carbonate Based Electrolytes for Si Anodes in Lithium Ion Batteries with NMR Spectroscopy, J. Am. Chem. Soc. 140 (2018) 9854–9867. doi:10.1021/jacs.8b03408.
[27] M. J. Frisch, G. W. Trucks, H. B. Schlegel, G. E. Scuseria, M. A. Robb, J. R. Cheeseman, G. Scalmani, V. Barone, B. Mennucci, G. A. Petersson, H. Nakatsuji, M. Caricato, X. Li, H. P. Hratchian, A. F. Izmaylov, J. Bloino, G. Zheng, J. L. Sonnenberg, M. Hada, M. Ehara, K. Toyota, R. Fukuda, J. Hasegawa, M. Ishida, T. Nakajima, Y. Honda, O. Kitao, H. Nakai, T. Vreven, J. A. Montgomery Jr, J. E. Peralta, F. Ogliaro, M. J. Bearpark, J. Heyd, E. N. Brothers, K. N. Kudin, V. N. Staroverov, R. Kobayashi, J. Normand, K. Raghavachari, A. P. Rendell, J. C. Burant, S. S. Iyengar, J. Tomasi, M. Cossi, N. Rega, N. J. Millam, M. Klene, J. E. Knox, J. B. Cross, V. Bakken, C. Adamo, J. Jaramillo, R. Gomperts, R. E. Stratmann, O. Yazyev, A. J. Austin, R. Cammi, C. Pomelli, J. W. Ochterski, R. L. Martin, K. Morokuma, V. G. Zakrzewski, G. A. Voth, P. Salvador, J. J. Dannenberg, S. Dapprich, A. D. Daniels, Ö. Farkas, J. B. Foresman, J. V. Ortiz, J. Cioslowski and D. J. Fox, Gaussian 16, Revision B.01, Gaussian, Inc., Wallingford, CT, USA, 2016.
[28] C. Forestier, P. Jankowski, A. Wizner, C. Davoisne, G. Gachot, L. Sannier, S. Grugeon, P. Johansson, M. Armand, S. Laruelle, Comparative investigation of solid electrolyte interphases created by the electrolyte additives vinyl ethylene carbonate and dicyano ketene vinyl ethylene acetal, J. Power Sources. 345 (2017) 212–220. doi:10.1016/j.jpowsour.2017.01.131.
[29] R.R. Hill, S.D. Rychnovsky, Generation, Stability, and Utility of Lithium 4,4'-Di- *tert* -butylbiphenylide (LiDBB), J. Org. Chem. 81 (2016) 10707–10714. doi:10.1021/acs.joc.6b01748.
[30] L. Gireaud, S. Grugeon, S. Laruelle, S. Pilard, J.-M. Tarascon, Identification of Li Battery Electrolyte Degradation Products Through Direct Synthesis and Characterization of Alkyl Carbonate Salts, J. Electrochem. Soc. 152 (2005) A850. doi:10.1149/1.1872673.

[31] K. Xu, G.V. Zhuang, J.L. Allen, U. Lee, S.S. Zhang, P.N. Ross,, T.R. Jow, Syntheses and Characterization of Lithium Alkyl Mono- and Dicarbonates as Components of Surface Films in Li-Ion Batteries, J. Phys. Chem. B. 110 (2006) 7708–7719. doi:10.1021/jp0601522.
[32] M. Armand, Matériaux d'Electrodes à Couple Redox Interne, PhD Diss. Univ. Joseph Fourier Ed. (1978).
[33] G.S. Lane, J.T. Miller, F.S. Modica, M.K. Barr, Infrared Spectroscopy of Adsorbed Carbon Monoxide on Platinum/Nonacidic Zeolite Catalysts, J. Catal. 141 (1993) 465–477. doi:https://doi.org/10.1006/jcat.1993.1155.
[34] T.C. Clarke, J.C. Scott, 13C NMR study of AsF5 doped polyacetylene, Solid State Commun. 41 (1982) 389–391. doi:10.1016/0038-1098(82)91185-1.
[35] N.S. Murthy, L.W. Shacklette, R.H. Baughman, Structure of lithium-doped polyacetylene, Phys. Rev. B. 40 (1989) 12550–12553. doi:10.1103/PhysRevB.40.12550.
[36] C. Forestier, S. Grugeon, C. Davoisne, A. Lecocq, G. Marlair, M. Armand, L. Sannier, S. Laruelle, Graphite electrode thermal behavior and solid electrolyte interphase investigations: Role of state-of-the-art binders, carbonate additives and lithium bis(fluorosulfonyl)imide salt, J. Power Sources. 330 (2016) 186–194. doi:10.1016/j.jpowsour.2016.09.005.
[37] H. Kim, S. Grugeon, G. Gachot, M. Armand, L. Sannier, S. Laruelle, Ethylene bis-carbonates as telltales of SEI and electrolyte health, role of carbonate type and new additives, Electrochimica Acta. 136 (2014) 157–165. doi:10.1016/j.electacta.2014.05.072.
[38] Y.-H. Liu, S. Takeda, I. Kaneko, H. Yoshitake, T. Mukai, M. Yanagida, Y. Saito, T. Sakai, Understanding the Improved High-Temperature Cycling Stability of a LiNi0.5Mn0.3Co0.2O2/Graphite Cell with Vinylene Carbonate: A Comprehensive Analysis Approach Utilizing LC-MS and DART-MS, J. Phys. Chem. C. 122 (2018) 5864–5870. doi:10.1021/acs.jpcc.7b10391.
[39] G. Gachot, S. Grugeon, M. Armand, S. Pilard, P. Guenot, J.-M. Tarascon, S. Laruelle, Deciphering the multi-step degradation mechanisms of carbonate-based electrolyte in Li batteries, J. Power Sources. 178 (2008) 409–421. doi:10.1016/j.jpowsour.2007.11.110.
[40] H.B. Son, M.-Y. Jeong, J.-G. Han, K. Kim, K.H. Kim, K.-M. Jeong, N.-S. Choi, Effect of reductive cyclic carbonate additives and linear carbonate co-solvents on fast chargeability of LiNi0.6Co0.2Mn0.2O2/graphite cells, J. Power Sources. 400 (2018) 147–156. doi:10.1016/j.jpowsour.2018.08.022.